Tuning Second Chern Number in a Four-Dimensional Topological Insulator by High-Frequency Time-Periodic Driving

Zheng-Rong Liu(刘峥嵘)[1], Rui Chen(陈锐)[1*], and Bin Zhou(周斌)[1,2*]

[1]*Department of Physics, Hubei University, Wuhan 430062, China*
[2]*Key Laboratory of Intelligent Sensing System and Security of Ministry of Education, Hubei University, Wuhan 430062, China*

(Received 20 January 2024; accepted manuscript online 18 March 2024)

Floquet engineering has attracted considerable attention as a promising approach for tuning topological phase transitions. We investigate the effects of high-frequency time-periodic driving in a four-dimensional (4D) topological insulator, focusing on topological phase transitions at the off-resonant quasienergy gap. The 4D topological insulator hosts gapless three-dimensional boundary states, characterized by the second Chern number C_2. We demonstrate that the second Chern number of 4D topological insulators can be modulated by tuning the amplitude of time-periodic driving. This includes transitions from a topological phase with $C_2 = \pm 3$ to another topological phase with $C_2 = \pm 1$, or to a topological phase with an even second Chern number $C_2 = \pm 2$, which is absent in the 4D static system. Finally, the approximation theory in the high-frequency limit further confirms the numerical conclusions.

DOI: 10.1088/0256-307X/41/4/047102

The discovery of the quantum Hall effect (QHE) opens the door to the field of topological matter.[1] In recent years, tremendous effort has been devoted to realizing the QHE in higher dimensions.[2–20] In 2001, Zhang and Hu proposed a four-dimensional (4D) generalization of the QHE.[21] The nth Chern numbers can characterize topological phases in $2n$ dimensions.[22–27] The 4D topological insulator (TI) exhibiting the 4D QHE supports fully gapped bulk and gapless three-dimensional (3D) boundary states, characterized by the second Chern number.[23,28–31] The 4D TI is impossible to realize in real materials due to the limitation of spatial dimensions. Consequently, various methods have been proposed to realize the 4D TIs in engineered systems. These include introducing synthetic dimensions in two-dimensional (2D) or 3D systems,[32–37] mapping high-dimensional models onto lower-dimensional systems,[38–43] and implementing 4D lattices by constructing appropriate capacitive and inductive connections in electric circuits.[26,44–46] Experimentally, 4D topological states have been realized in various systems such as acoustic lattices,[34] photonic crystals,[35,39,47] an angled optical superlattice with ultracold bosonic atoms,[38] and electric circuits.[26,44–46]

The modulation of topological phases has emerged as a significant topic in condensed matter physics.[48–53] Recently, Floquet engineering, the manipulation of quantum systems through time-periodic driving, has been widely investigated in lower-dimensional ($d \leq 3$) systems.[54–79] Floquet engineering has been successfully employed in emulating the Thouless pump with quantized energy as opposed to charge,[80] and serving as a technique to induce novel topological states from initially trivial states.[57,81–88] Up to date, numerous researches on periodically driven topological states have been reported in various systems, including solid-state materials,[57–61,83,89–94] photonic crystals,[62,86,95–101] acoustic lattices,[102–105] electric circuits,[106] and cold atom systems.[107–110] Motivated by the above-mentioned researches, a question whether time-periodic driving can modulate topological phase transitions in 4D TIs naturally arises.

In this work, we present a systematic study on the time-periodically driven 4D TI with a high-frequency time-periodic driving. Here, we only focus on the high-frequency case where the frequency of the time-periodic driving is greater than the bandwidth of the static system, and there is no overlap between the undriven quasienergy bands and the driven quasienergy bands. We consider a 4D time-periodic vector potential $\boldsymbol{V}$ (V_x, V_y, V_z, V_w) as the time-periodic driving. When $V_x \neq 0$ or $V = V_n \neq 0$ $(n = x, y, z, w)$, the second Chern number of the 4D system can be changed by tuning the amplitude of the time-periodic driving. Moreover, when $V_x = V_y \neq 0$ or $V_x = V_y = V_z \neq 0$, one can find that the time-periodic driving transforms a topological phase with $C_2 = \pm 3$ to another topological phase with $C_2 = \pm 1$, or to a topological phase with an even second Chern number $C_2 = \pm 2$, which is absent in the 4D static system. Furthermore, the phase diagram of the 4D Floquet system is explained by using the high-frequency approximation method.

Static Model. The Dirac model describing the 4D TI is given by the following equation:[23]

$$H(\boldsymbol{k}) = \Gamma_2 \sin k_x + \Gamma_3 \sin k_y + \Gamma_4 \sin k_z + \Gamma_5 \sin k_w + \Gamma_1 m(\boldsymbol{k}), \quad (1)$$

*Corresponding authors. Email: chenr@hubu.edu.cn; binzhou@hubu.edu.cn
© 2024 Chinese Physical Society and IOP Publishing Ltd

where the Dirac matrices $\Gamma_j = (s_x \otimes s_0,\ s_y \otimes s_0,\ s_z \otimes s_x,\ s_z \otimes s_y,\ s_z \otimes s_z)$, $j = 1, 2, 3, 4, 5$, satisfying the anticommutation relations $\{\Gamma_i, \Gamma_j\} = 2\delta_{ij}$; $m(\boldsymbol{k}) = m + c(\cos k_x + \cos k_y + \cos k_z + \cos k_w)$, where m is the Dirac mass and c denotes the nearest-neighbor hopping amplitude. In subsequent calculations, $c = 1$. The doubly degenerate eigenvalues of $H(\boldsymbol{k})$ are

$$E(\boldsymbol{k}) = \pm\frac{1}{\sqrt{2}}\sqrt{4+2[m(\boldsymbol{k})]^2-\sum\nolimits_{n=x,y,z,w}\cos(2k_n)}, \quad (2)$$

and the bandwidth of the system is $E_{\mathrm{W}} = 2|m| + 8$. In Fig. 1(a), we plot the bulk gap E_{g} with respect to the Dirac mass m. Remarkably, the bulk gap E_{g} is closed at $m = \pm 4$, $m = \pm 2$, $m = 0$.

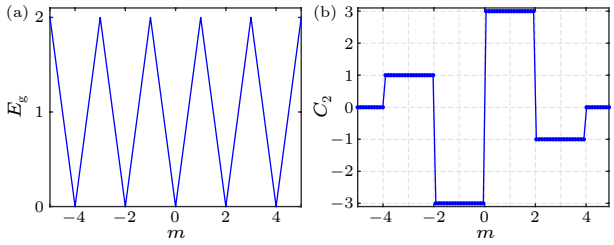

Fig. 1. (a) The bulk gap E_{g} as a function of the parameter m. (b) The second Chern number C_2 as a function of the parameter m.

Second Chern Number. The second Chern number is used to describe the nonlinear response of the current to an electric field and a magnetic field in the 4D TI.[21] It is given by the following formula:[23–25,111,112]

$$C_2 = \frac{1}{4\pi^2}\int_{\mathrm{FBZ}} d\boldsymbol{k}\mathrm{Tr}[F_{xy}F_{zw} + F_{wx}F_{zy} + F_{zx}F_{yw}], \quad (3)$$

with the non-Abelian Berry curvature

$$F^{\alpha\beta}_{mn} = \partial_m A^{\alpha\beta}_n - \partial_n A^{\alpha\beta}_m + i[A_m,\ A_n]^{\alpha\beta}, \quad (4)$$

where $m, n = x, y, z, w$ and the Berry connection of the occupied bands $A^{\alpha\beta}_m = -i\left\langle u^{\alpha}(\boldsymbol{k})\right| \frac{\partial}{\partial k_m}\left|u^{\beta}(\boldsymbol{k})\right\rangle$, and $|u^{\alpha}(\boldsymbol{k})\rangle$ denotes the occupied eigenstates with $\alpha = 1, \ldots, N_{\mathrm{occ}}$.

Figure 1(b) shows the second Chern number C_2 as a function of the Dirac mass m. It is obvious that the phase transition of the system is accompanied by the closure of the bulk gap. In the region $-4 < m < -2$, the second Chern number $C_2 = 1$. In the first Brillouin zone (FBZ) of the quasi-3D system [open boundary conditions (OBC) along the x direction], there is a single gapless Dirac cone cross at the point $G = (k_y = 0, k_z = 0, k_w = 0)$ as shown in Fig. 2(a). In the region $-2 < m < 0$, the second Chern number $C_2 = -3$. There are three gapless Dirac cones cross at the points $Y = (\pi, 0, 0)$, $Z = (0, \pi, 0)$, and $W = (0, 0, \pi)$ [Fig. 2(b)]. The results for $m > 0$ are symmetrically distributed with those for $m < 0$. In the region $0 < m < 2$, the second Chern number $C_2 = 3$. There are three gapless Dirac cones cross at the points $M_{yz} = (\pi, \pi, 0)$, $M_{yw} = (\pi, 0, \pi)$, and $M_{zw} = (0, \pi, \pi)$ [Fig. 2(c)]. Finally, in the region $2 < m < 4$, the second Chern number $C_2 = -1$. There is one gapless Dirac cone cross at the vertex of the FBZ $R = (\pi, \pi, \pi)$ [Fig. 2(d)].

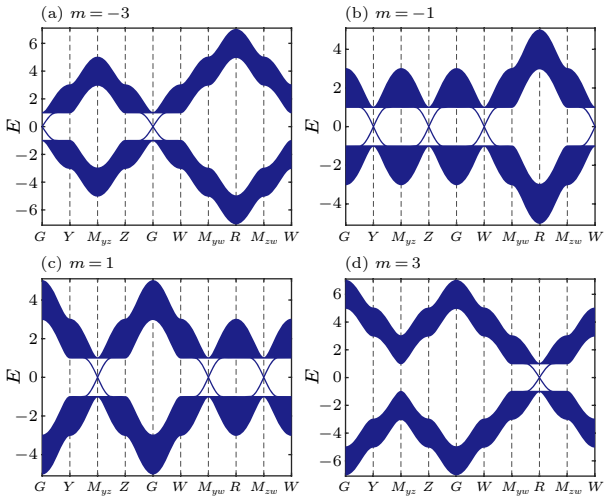

Fig. 2. Energy spectra for (a) $m = -3$, (b) $m = -1$, (c) $m = 1$, and (d) $m = 3$ when the OBC along the x direction. The horizontal axis shows the high symmetry points in the FBZ of the quasi-3D system, $G = (k_y = 0, k_z = 0, k_w = 0)$, $Y = (\pi, 0, 0)$, $Z = (0, \pi, 0)$, $W = (0, 0, \pi)$, $M_{yz} = (\pi, \pi, 0)$, $M_{yw} = (\pi, 0, \pi)$, $M_{zw} = (0, \pi, \pi)$, $R = (\pi, \pi, \pi)$.

Time-Periodically Driven Model and Floquet Hamiltonian. The Floquet theory is often used to study time-periodic systems.[113,114] For a time-periodic Hamiltonian $H(\tau) = H(\tau + T)$ with the period $T = 2\pi/\omega$ (ω is the frequency), the wave function $\Psi_\alpha(\tau) = e^{-i\varepsilon_\alpha \tau}\psi_\alpha$ of the Schrödinger equation $i\partial_\tau\Psi(\tau) = H(\tau)\Psi(\tau)$ can be obtained by employing the Floquet theory, where ε_α is the α-th quasienergy. Using the Fourier transformation, the time-dependent Schrödinger equation can be converted into a time-independent Schrödinger equation:

$$H_{\mathrm{F}}\psi_\alpha = \varepsilon_\alpha\psi_\alpha, \quad (5)$$

where

$$\begin{aligned} H_{\mathrm{F},qp} &= q\omega\delta_{qp}I + H_{p-q}, \\ H_0 &= \frac{1}{T}\int_0^T d\tau H(\tau), \\ H_{p-q} &= \frac{1}{T}\int_0^T d\tau H(\tau)e^{i(p-q)\omega\tau}, \end{aligned} \quad (6)$$

I is an identity matrix of the same size as $H(\tau)$; p, q take $0, \pm 1, \pm 2, \ldots$ and the Floquet Hamiltonian H_{F} is an infinite Hamiltonian. In the numerical calculations, p and q are taken to be finite integers until the results converge. When $\omega > E_{\mathrm{W}}$, there is no overlap between quasienergy bands at different intervals $\varepsilon \in [(n - 1/2)\omega, (n + 1/2)\omega]$, and n is an integer. In the subsequent content, we restrict our attention to the quasienergy interval $\varepsilon \in [-\omega/2, \omega/2]$.

We apply the time-periodic vector potential $\boldsymbol{V}(V_x, V_y, V_z, V_w)$ to the 4D Dirac model $H(\boldsymbol{k})$, then the time-dependent Hamiltonian $H(\boldsymbol{k}, \tau)$ is given by the following expression:

$$H(\boldsymbol{k}, \tau) = \sum_{j=1}^{5} h_j(\boldsymbol{k}, \tau)\Gamma_j, \quad (7)$$

with

$$\begin{aligned} h_1(\boldsymbol{k},\tau) &= m + c\sum_{n=x,y,z,w}\cos[k_n + V_n\cos(\omega\tau)],\\ h_2(\boldsymbol{k},\tau) &= \sin[k_x + V_x\cos(\omega\tau)],\\ h_3(\boldsymbol{k},\tau) &= \sin[k_y + V_y\cos(\omega\tau)],\\ h_4(\boldsymbol{k},\tau) &= \sin[k_z + V_z\cos(\omega\tau)],\\ h_5(\boldsymbol{k},\tau) &= \sin[k_w + V_w\cos(\omega\tau)], \end{aligned} \tag{8}$$

where V_n $(n = x, y, z, w)$ is the amplitude of the time-periodic vector potential. After the Fourier transformation, the diagonal component in the Floquet Hamiltonian $H_{\rm F}$ is expressed as follows:

$$H_0 = \sum_{j=1}^{5} h_{0,j}\Gamma_j, \tag{9}$$

with

$$\begin{aligned} h_{0,1} &= m + c\sum_{n=x,y,z,w}\cos(k_n)\mathcal{J}_0(V_n),\\ h_{0,2} &= \sin k_x\mathcal{J}_0(V_x), \quad h_{0,3} = \sin k_y\mathcal{J}_0(V_y),\\ h_{0,4} &= \sin k_z\mathcal{J}_0(V_z), \quad h_{0,5} = \sin k_w\mathcal{J}_0(V_w), \end{aligned} \tag{10}$$

and the off-diagonal components are

$$H_{-l} = \sum_{j=1}^{5} h_{-l,j}\Gamma_j, H_{+l} = H_{-l}^{\dagger}, \tag{11}$$

with

$$\begin{aligned} h_{-l,1} &= \frac{c}{2}\sum_{n=x,y,z,w}\left[e^{ik_n} + (-1)^l e^{-ik_n}\right]\mathcal{J}_l(V_n),\\ h_{-l,2} &= -\frac{i}{2}\left[e^{ik_x} - (-1)^l e^{-ik_x}\right]\mathcal{J}_l(V_x),\\ h_{-l,3} &= -\frac{i}{2}\left[e^{ik_y} - (-1)^l e^{-ik_y}\right]\mathcal{J}_l(V_y),\\ h_{-l,4} &= -\frac{i}{2}\left[e^{ik_z} - (-1)^l e^{-ik_z}\right]\mathcal{J}_l(V_z),\\ h_{-l,5} &= -\frac{i}{2}\left[e^{ik_w} - (-1)^l e^{-ik_w}\right]\mathcal{J}_l(V_w), \end{aligned} \tag{12}$$

where $\mathcal{J}_l(V_n)$ is the l-th Bessel function of the first kind, $l = |p - q|$ $(p \neq q)$. Then, the Floquet Hamiltonian $H_{\rm F}$ is given by the following matrix:

$$H_{\rm F} = \begin{pmatrix} \ddots & \vdots & \vdots & \vdots & \ddots \\ \cdots & H_0 - \omega & H_{+1} & H_{+2} & \cdots \\ \cdots & H_{-1} & H_0 & H_{+1} & \cdots \\ \cdots & H_{-2} & H_{-1} & H_0 + \omega & \cdots \\ \ddots & \vdots & \vdots & \vdots & \ddots \end{pmatrix}. \tag{13}$$

The band of the diagonal component H_0 $(H_0 \pm \omega)$ is referred to as the undriven (driven) band. The driven and undriven bands do not overlap when the frequency ω is greater than the bandwidth of the static system $E_{\rm W} = 2|m| + 8$, so we only focus on topological phase transitions in the off-resonant quasienergy gap in the subsequent discussion.

Time-Periodic Driving $\boldsymbol{V}(V_x, 0, 0, 0)$. We first consider the time-periodic driving $\boldsymbol{V}(V_x, 0, 0, 0)$. Then, the diagonal component in the Floquet Hamiltonian $H_{\rm F}$ is given by

$$H_0 = \sum_{j=1}^{5} h_{0,j}\Gamma_j, \tag{14}$$

with

$$\begin{aligned} h_{0,1} &= m + c[\cos k_x\mathcal{J}_0(V_x)\\ &\quad + \cos k_y + \cos k_z + \cos k_w],\\ h_{0,2} &= \sin k_x\mathcal{J}_0(V_x), \quad h_{0,3} = \sin k_y,\\ h_{0,4} &= \sin k_z, \quad h_{0,5} = \sin k_w, \end{aligned} \tag{15}$$

and the off-diagonal components are

$$H_{-l} = \sum_{j=1}^{5} h_{-l,j}\Gamma_j, \quad H_{+l} = H_{-l}^{\dagger}, \tag{16}$$

with

$$\begin{aligned} h_{-l,1} &= \frac{c}{2}\left[e^{ik_x} + (-1)^l e^{-ik_x}\right]\mathcal{J}_l(V_x),\\ h_{-l,2} &= -\frac{i}{2}\left[e^{ik_x} - (-1)^l e^{-ik_x}\right]\mathcal{J}_l(V_x),\\ h_{-l,3} &= h_{-l,4} = h_{-l,5} = 0. \end{aligned} \tag{17}$$

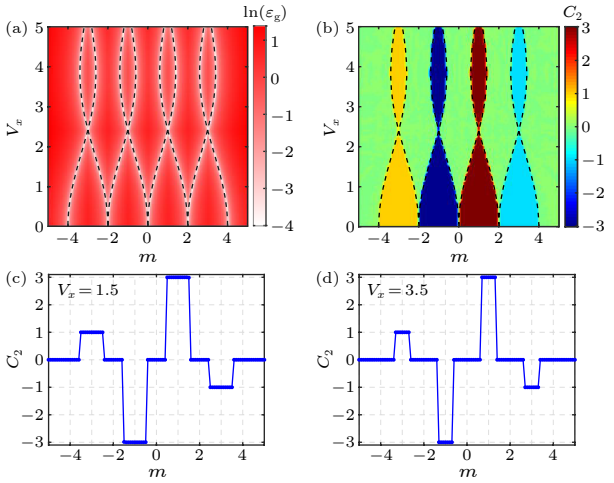

Fig. 3. (a) The logarithm of the bulk gap $\ln(\varepsilon_{\rm g})$ as a function of m and V_x. The white area indicates that the bulk gap is close to zero, and black dashed lines are given by $m = \pm 3 \pm \mathcal{J}_0(V_x)$, $m = \pm 1 \pm \mathcal{J}_0(V_x)$. (b) Second Chern number C_2 as a function of m and V_x. [(c), (d)] The second Chern number C_2 as a function of the parameter m for (c) $V_x = 1.5$ and (d) $V_x = 3.5$.

By numerically diagonalizing the Floquet Hamiltonian $H_{\rm F}$, we show the logarithm of the bulk gap as a function of m and V_x in Fig. 3(a). Here, the bulk gap refers to the quasienergy gap near $\varepsilon = 0$. The color bar converging to white represents the bulk gap close to 0. In the high-frequency limit (i.e., $\omega \gg E_{\rm W}$), we can obtain the effective Floquet Hamiltonian $H_{\rm eff}$. The black dashed lines in Fig. 3(a) can be given by solving the effective Hamiltonian, $m = \pm 3 \pm \mathcal{J}_0(V_x)$, $m = \pm 1 \pm \mathcal{J}_0(V_x)$ (see the Supplemental Material for details). Obviously, the results obtained by solving numerically for the Floquet Hamiltonian $H_{\rm F}$ are consistent with those obtained by solving analytically for the effective Hamiltonian $H_{\rm eff}$.

Accordingly, we plot the phase diagram of the system as a function of m and V_x in Fig. 3(b). It is found that as the amplitude of the periodic driving V_x increases, the topologically nontrivial regions with nonzero second Chern numbers diminish until they completely vanish at $\mathcal{J}_0(V_{x,c}) = 0$. However, when $V_x > V_{x,c} \approx 2.405$, the topologically nontrivial phase of the system reappears. Figures 3(c) and 3(d) show the second Chern number as a function of the Dirac mass m when $V_x < V_{x,c}$ and $V_x > V_{x,c}$, respectively. It is found that the reappeared topologically nontrivial phase exhibits the same second Chern number as before the phase transition. Figure 4 illustrates the quasienergy spectra of different topologically nontrivial phases at $V_x = 3.5$ when the OBC along the x direction. The right panels show the quasienergy spectra in the interval $[-\omega/2, \omega/2]$. The results of the system with OBC along the y, z, or w direction are the same as the result in Fig. 4, i.e., the number of gapless 3D topological boundary states is equal to the value of the second Chern number. Here, we only discuss the topological phase transitions for $V_x \neq 0$. It should be noted that topological phase transitions for $V_n \neq 0$ ($n = y$, z, or w) is similar to those presented here.

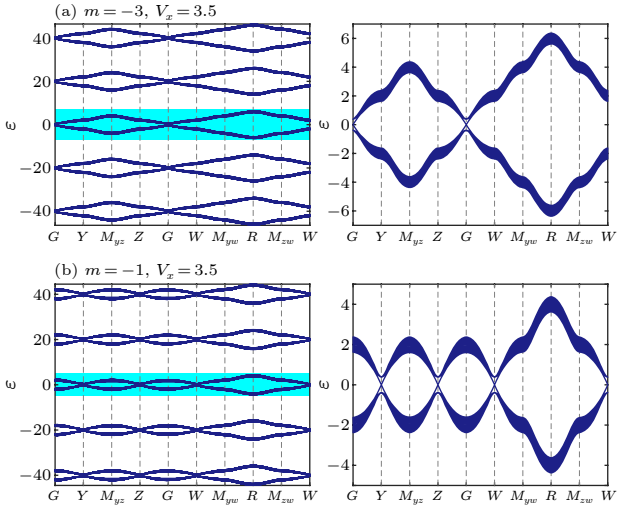

Fig. 4. [(a), (b)]Quasienergy spectra for (a) $m = -3$ and (b) $m = -1$ when the OBC along the x direction. The horizontal axis shows the high symmetry points in the FBZ of the quasi-3D system, G = ($k_y = 0$, $k_z = 0$, $k_w = 0$), Y = (π, 0, 0), Z = (0, π, 0), W = (0, 0, π), M_{yz} = (π, π, 0), M_{yw} = (π, 0, π), M_{zw} = (0, π, π), R = (π, π, π). The right panels show the cyan area of the left panels. The amplitude and frequency of the periodic driving are $V_x = 3.5$ and $\omega = 20$.

Topological Phases with Even Second Chern Number. We consider the periodic driving $\boldsymbol{V}(V_x, V_y, 0, 0)$, where $V_x = V_y = V_{xy} \neq 0$. Then, the diagonal component in the Floquet Hamiltonian $H_{\rm F}$ is given by

$$H_0 = \mathcal{J}_0(V_{xy})\Gamma_2 \sin k_x + \mathcal{J}_0(V_{xy})\Gamma_3 \sin k_y + \Gamma_4 \sin k_z + \Gamma_5 \sin k_w + \Gamma_1 m(\boldsymbol{k}), \tag{18}$$

and the off-diagonal components are

$$H_{-l} = \sum_{j=1}^{5} h_{-l,j}\Gamma_j, \quad H_{+l} = H_{-l}^{\dagger}, \tag{19}$$

with

$$\begin{aligned} h_{-l,1} &= \frac{c}{2}[e^{ik_x} + (-1)^l e^{-ik_x} + e^{ik_y} + (-1)^l e^{-ik_y}]\mathcal{J}_l(V_{xy}), \\ h_{-l,2} &= -\frac{i}{2}[e^{ik_x} - (-1)^l e^{-ik_x}]\mathcal{J}_l(V_{xy}), \\ h_{-l,3} &= -\frac{i}{2}[e^{ik_y} - (-1)^l e^{-ik_y}]\mathcal{J}_l(V_{xy}), \\ h_{-l,4} &= h_{-l,5} = 0, \end{aligned} \tag{20}$$

where $m(\boldsymbol{k}) = m + c[\mathcal{J}_0(V_{xy})\cos k_x + \mathcal{J}_0(V_{xy})\cos k_y + \cos k_z + \cos k_w]$. By numerically diagonalizing the Floquet Hamiltonian $H_{\rm F}$, we show the bulk gap as a function of m and V_{xy} in Fig. 5(a), where the white region signifies the bulk gap close to zero. Then, we derive the effective Hamiltonian $H_{\rm eff}$ for this system based on the Floquet theory in the high-frequency limit (see the Supplemental Material for details). By analytically solving for the effective Hamiltonian $H_{\rm eff}$, we can obtain the black dashed lines in Fig. 5(a). The black dashed lines correspond to points where the bulk gap is zero, given by $m = 0$, $m = \pm 2$, $m = \pm 2\mathcal{J}_0(V_{xy})$, and $m = \pm 2 \pm 2\mathcal{J}_0(V_{xy})$. These black dashed lines fit well with the numerical calculations for the Floquet Hamiltonian.

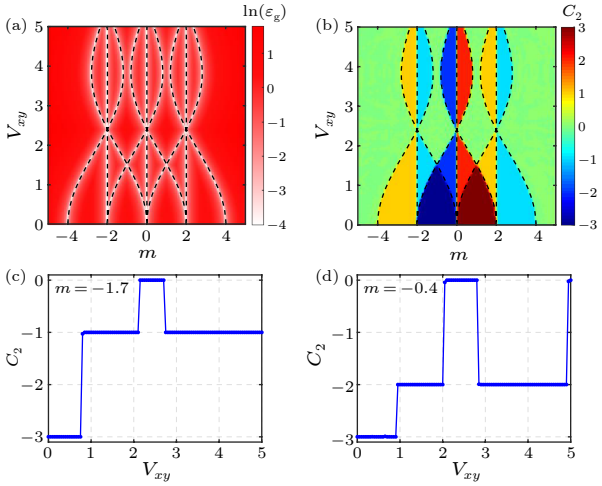

Fig. 5. (a) The logarithm of the bulk gap as a function of m and V_{xy}. The white area indicates that the bulk gap is close to zero, and black dashed lines are given by $m = 0$, $m = \pm 2$, $m = \pm 2\mathcal{J}_0(V_{xy})$, and $m = \pm 2 \pm 2\mathcal{J}_0(V_{xy})$. (b) Second Chern number C_2 as a function of m and V_{xy}. [(c), (d)] The second Chern number C_2 as a function of V_{xy} for (c) $m = -1.7$ and (d) $m = -0.4$.

In Fig. 5(b), we show the phase diagram in the (m, V_{xy}) plane. The color map corresponds to the value of the second Chern number. Notably, the position of the phase transition point coincides with that of the closure point in the bulk gap. In the range of $1 < |m| < 2$, it can be observed that as the amplitude of the time-periodic driving V_{xy} increases, the system undergoes a phase transition from a topological phase with $C_2 = -3$ to another topological phase with $C_2 = -1$ as shown in Fig. 5(c). The quasienergy spectra of the quasi-3D system are shown in Figs. 6(a) and 6(b). It is evident that the time-periodic driving V_{xy} induces the emergence of the topological phase with $C_2 = -1$, distinguished by a single gapless Dirac

point. When $V_{xy} = 1.5$ ($V_{xy} = 3.5$), this Dirac point is located at the point Y ($k_y = \pi$, $k_z = 0$, $k_w = 0$) [G (0, 0, 0)].

Moreover, it is intriguing that for $|m| < 1$, the periodic driving can induce the emergence of a topologically nontrivial system with an even second Chern number $C_2 = \pm 2$. Figure 5(d) illustrates the second Chern number C_2 as a function of the amplitude V_{xy} when $m = -0.4$. When the amplitude V_{xy} exceeds the critical value $V_{xy,c} = 0.9184$, the system transitions from the topological phase with $C_2 = -3$ to another topological phase with $C_2 = -2$. Within the interval $0.9184 < V_{xy} < 2.0415$, C_2 keeps a quantized plateau with $C_2 = -2$. As shown in Fig. 6(c), there are two Dirac points in the FBZ of the quasi-3D system at points Z ($k_y = 0$, $k_z = \pi$, $k_w = 0$) and W ($k_y = 0$, $k_z = 0$, $k_w = \pi$). When $V_{xy} > 2.0415$, the topological properties of the system are destroyed until $V_{xy} > 2.8371$. In the interval $V_{xy} \in (2.8371, 4.9307)$, the topologically nontrivial phase with the second Chern number $C_2 = -2$ reemerges. In this case, there are two Dirac points in the FBZ as shown in Fig. 6(d). It is noteworthy that in these topologically nontrivial systems induced by V_{xy}, when the OBC along the z or w direction, the value of the second Chern number does not coincide with the number of Dirac points (see the Supplemental Material for details).

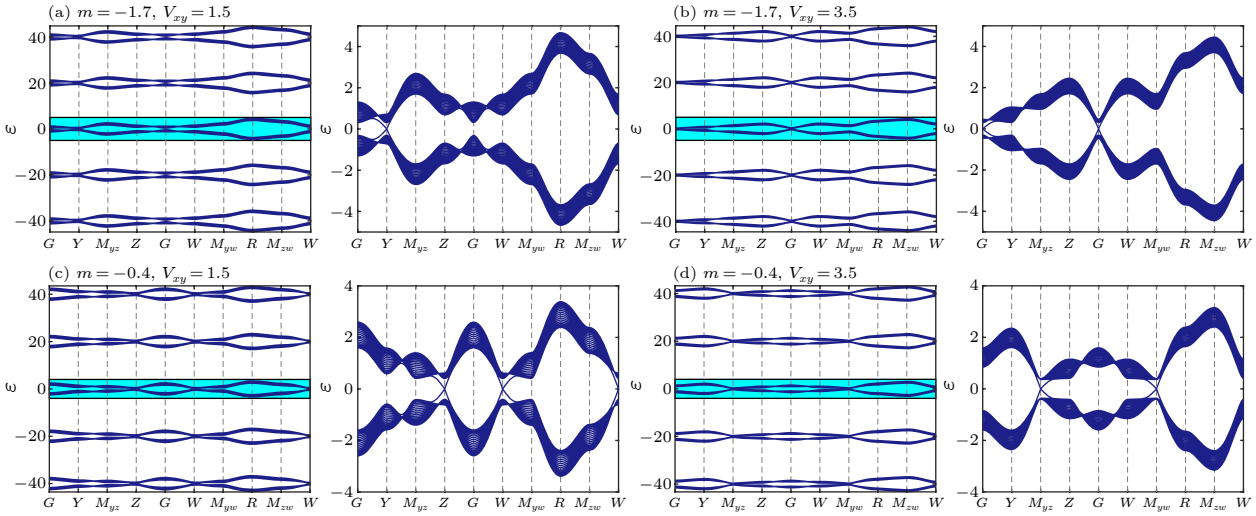

Fig. 6. Quasienergy spectra for the OBC along the x direction. The horizontal axis shows the high symmetry points in the FBZ of the quasi-3D system, $G = (k_y = 0, k_z = 0, k_w = 0)$, $Y = (\pi, 0, 0)$, $Z = (0, \pi, 0)$, $W = (0, 0, \pi)$, $M_{yz} = (\pi, \pi, 0)$, $M_{yw} = (\pi, 0, \pi)$, $M_{zw} = (0, \pi, \pi)$, $R = (\pi, \pi, \pi)$. The right panels show the cyan area of the left panels. The Dirac mass and the amplitude of the periodic driving are $m = -1.7$ and $V_{xy} = 1.5$ for (a), $m = -1.7$ and $V_{xy} = 3.5$ for (b), $m = -0.4$ and $V_{xy} = 1.5$ for (c), $m = -0.4$ and $V_{xy} = 3.5$ for (d). Here, we choose $\omega = 20$.

Conclusion and Discussion. In this work, we investigate the effects of high-frequency time-periodic driving in a 4D TI. First, we find that the time-periodic driving $\boldsymbol{V}(V_x, 0, 0, 0)$ can modulate the topological phase of the 4D TI when $V_x \neq 0$. By tuning the amplitude of the time-periodic driving of $\boldsymbol{V}(V_x, 0, 0, 0)$, the size of the topologically nontrivial regions with nonzero second Chern numbers can be modified. Additionally, the topologically nontrivial regions vanish when $\mathcal{J}_0(V_{x,c}) = 0$. The Floquet system exhibits similar results when $V = V_n \neq 0$ ($n = x, y, z, w$) (see the Supplemental Material for more details). In addition, we show that the time-periodic driving $\boldsymbol{V}(V_x, V_y, 0, 0)$ can force the system to convert from a topological phase with $C_2 = \pm 3$ to another topological phase with $C_2 = \pm 1$. When the Dirac mass $|m| < 1$, the periodic driving V_{xy} can additionally induce a topological phase characterized by an even second Chern number $C_2 = \pm 2$. Note that there is no such topologically nontrivial phase with an even second Chern number in the 4D static system. Similarly, the time-periodic driving $\boldsymbol{V}(V_x, V_y, V_z, 0)$ can also induce a topologically nontrivial phase with $C_2 = \pm 2$ (see the Supplemental Material). Furthermore, the Floquet phase diagram can be explained by the approximation theory in the high-frequency limit.

Experimentally, electronic circuits can be used to realize the 4D system.[44,45] With tunable complex-phase elements, momentum components of the 4D Dirac model can be periodically driven to realize the time-dependent Hamiltonian.[46] Therefore, we expect that the time-periodically driven 4D TIs can be experimentally realized through topolectrical circuit networks.

Moreover, we wish to emphasize the difference between this work and our previous work.[115] This work is fundamentally different from the previous work for the following two reasons: (i) In the previous work, we studied the effects of time-periodic driving on a 4D normal insulator, while in this work, we focus on a 4D topological insulator. (ii) In the previous work, the frequency of the time-periodic driving is smaller than the bandwidth of the static system, so we only focused on topological phase transitions at the resonant quasienergy gap. In this work, we focus on topological phase transitions at the off-resonant quasienergy gap.

Acknowledgments. This work was supported by the National Natural Science Foundation of China (Grant Nos. 12074107 and 12304195), the Program of Outstanding

Young and Middle-Aged Scientific and Technological Innovation Team of Colleges and Universities in Hubei Province (Grant No. T2020001), and the Innovation Group Project of the Natural Science Foundation of Hubei Province of China (Grant No. 2022CFA012), the Chutian Scholars Program in Hubei Province, the Postdoctoral Fellowship Program of CPSF (Grant No. GZC20230751), and the Postdoctoral Innovation Research Program in Hubei Province (Grant No. 351342).

References

[1] Klitzing K V, Dorda G, and Pepper M 1980 *Phys. Rev. Lett.* **45** 494
[2] Shen S Q 2017 *Topological Insulators* (Singapore: Springer)
[3] Wang C M, Sun H P, Lu H Z, and Xie X C 2017 *Phys. Rev. Lett.* **119** 136806
[4] Zhang C, Zhang Y, Yuan X, Lu S, Zhang J, Narayan A, Liu Y, Zhang H, Ni Z, Liu R, Choi E S, Suslov A, Sanvito S, Pi L, Lu H Z, Potter A C, and Xiu F 2018 *Nature* **565** 331
[5] Tang F D, Ren Y F, Wang P P, Zhong R D, Schneeloch J, Yang S A, Yang K, Lee P A, Gu G, Qiao Z, and Zhang L 2019 *Nature* **569** 537
[6] Chen R, Liu T, Wang C M, Lu H Z, and Xie X C 2021 *Phys. Rev. Lett.* **127** 066801
[7] Qin F, Li S, Du Z Z, Wang C M, Zhang W, Yu D, Lu H Z, and Xie X C 2020 *Phys. Rev. Lett.* **125** 206601
[8] Störmer H L, Eisenstein J P, Gossard A C, Wiegmann W, and Baldwin K 1986 *Phys. Rev. Lett.* **56** 85
[9] Hannahs S T, Brooks J S, Kang W, Chiang L Y, and Chaikin P M 1989 *Phys. Rev. Lett.* **63** 1988
[10] Montambaux G and Kohmoto M 1990 *Phys. Rev. B* **41** 11417
[11] Kohmoto M, Halperin B I, and Wu Y S 1992 *Phys. Rev. B* **45** 13488
[12] Hill S, Uji S, Takashita M, Terakura C, Terashima T, Aoki H, Brooks J S, Fisk Z, and Sarrao J 1998 *Phys. Rev. B* **58** 10778
[13] Koshino M, Aoki H, Kuroki K, Kagoshima S, and Osada T 2001 *Phys. Rev. Lett.* **86** 1062
[14] Bernevig B A, Hughes T L, Raghu S, and Arovas D P 2007 *Phys. Rev. Lett.* **99** 146804
[15] Masuda H, Sakai H, Tokunaga M, Yamasaki Y, Miyake A, Shiogai J, Nakamura S, Awaji S, Tsukazaki A, Nakao H, Murakami Y, Arima T H, Tokura Y, and Ishiwata S 2016 *Sci. Adv.* **2** e1501117
[16] Jin Y J, Wang R, Xia B W, Zheng B B, and Xu H 2018 *Phys. Rev. B* **98** 081101
[17] Li H L, Liu H W, Jiang H, and Xie X C 2020 *Phys. Rev. Lett.* **125** 036602
[18] Cheng S G, Jiang H, Sun Q F, and Xie X C 2020 *Phys. Rev. B* **102** 075304
[19] Wang P, Ren Y, Tang F, Wang P P, Hou T, Zeng H L, Zhang L Y, and Qiao Z H 2020 *Phys. Rev. B* **101** 161201
[20] Li S, Wang C M, Du Z Z, Qin F, Lu H Z, and Xie X C 2021 *npj Quantum Mater.* **6** 96
[21] Zhang S C and Hu J 2001 *Science* **294** 823
[22] Bernevig B A and Hughes T L 2013 *Topological Insulators and Topological Superconductors* (Princeton: Princeton University Press)
[23] Qi X L, Hughes T L, and Zhang S C 2008 *Phys. Rev. B* **78** 195424
[24] Mochol-Grzelak M, Dauphin A, Celi A, and Lewenstein M 2018 *Quantum Sci. Technol.* **4** 014009
[25] Sugawa S, Salces-Carcoba F, Perry A R, Yue Y, and Spielman I B 2018 *Science* **360** 1429
[26] Zhang W X, Di F X, Zheng X G, Sun H J, and Zhang X D 2023 *Nat. Commun.* **14** 1083
[27] Bouhon A, Zhu Y Q, Slager R J, and Palumbo G 2023 arXiv:2301.08827v1 [cond-mat.mes-hall]
[28] Li Y, Zhang S C, and Wu C 2013 *Phys. Rev. Lett.* **111** 186803
[29] Zhu Y Q, Zheng Z, Palumbo G, and Wang Z D 2022 *Phys. Rev. Lett.* **129** 196602
[30] Terrier F and Kunst F K 2020 *Phys. Rev. Res.* **2** 023364
[31] Chen R, Yi X X, and Zhou B 2023 *Phys. Rev. B* **108** 085306
[32] Price H M, Zilberberg O, Ozawa T, Carusotto I, and Goldman N 2015 *Phys. Rev. Lett.* **115** 195303
[33] Ozawa T, Price H M, Goldman N, Zilberberg O, and Carusotto I 2016 *Phys. Rev. A* **93** 043827
[34] Chen Z G, Zhu W, Tan Y, Wang L, and Ma G 2021 *Phys. Rev. X* **11** 011016
[35] Chen X D, Shi F L, Liu J W, Shen K, He X T, Chan C T, Chen W J, and Dong J W 2022 *Nat. Sci. Rev.* **10** nwac289
[36] Kim K W, Bagrets D, Micklitz T, and Altland A 2023 *Phys. Rev. X* **13** 011003
[37] Peng Y and Refael G 2018 *Phys. Rev. B* **97** 134303
[38] Lohse M, Schweizer C, Price H M, Zilberberg O, and Bloch I 2018 *Nature* **553** 55
[39] Zilberberg O, Huang S, Guglielmon J, Wang M, Chen K P, Kraus Y E, and Rechtsman M C 2018 *Nature* **553** 59
[40] Kraus Y E, Ringel Z, and Zilberberg O 2013 *Phys. Rev. Lett.* **111** 226401
[41] Edge J M, Tworzydło J, and Beenakker C W J 2012 *Phys. Rev. Lett.* **109** 135701
[42] Lee C H, Wang Y, Chen Y, and Zhang X 2018 *Phys. Rev. B* **98** 094434
[43] Petrides I, Price H M, and Zilberberg O 2018 *Phys. Rev. B* **98** 125431
[44] Wang Y, Price H M, Zhang B, and Chong Y D 2020 *Nat. Commun.* **11** 2356
[45] Yu R, Zhao Y X, and Schnyder A P 2020 *Nat. Sci. Rev.* **7** 1288
[46] Chen A, Brand H, Helbig T, Hofmann T, Imhof S, Fritzsche A, KieBling T, Stegmaier A, Upreti L K, Neupert T, Bzdušek T, Greiter M, Thomale R, and Boettcher I 2023 *Nat. Commun.* **14** 622
[47] Liu H, Lai P, Wang H, Cheng H, Tian J, and Chen S 2023 *Nanophotonics* **12** 2273
[48] Jin L and Song Z 2019 *Phys. Rev. B* **99** 081103
[49] Shen J L, Yao Q S, Zeng Q Q, Sun H Y, Xi X K, Wu G H, Wang W H, Shen B G, Liu Q H, and Liu E K 2020 *Phys. Rev. Lett.* **125** 086602
[50] Wu H C, Jin L, and Song Z 2021 *Phys. Rev. B* **103** 235110
[51] Ma Z, Liu Y, Xie Y X, and Wang Y S 2023 *Phys. Rev. Appl.* **19** 054038
[52] Jin K H, Jiang W, Sethi G, and Liu F 2023 *Nanoscale* **15** 12787
[53] Wu H C, Xu H S, Xie L C, and Jin L 2024 *Phys. Rev. Lett.* **132** 083801
[54] Dahlhaus J P, Fregoso B M, and Moore J E 2015 *Phys. Rev. Lett.* **114** 246802
[55] Kaladzhyan V, Simon P, and Trif M 2017 *Phys. Rev. B* **96** 020507
[56] Sie E J, McIver J W, Lee Y H, Fu L, Kong J, and Gedik N 2015 *Nat. Mater.* **14** 290
[57] Lindner N H, Refael G, and Galitski V 2011 *Nat. Phys.* **7** 490
[58] Wang Y H, Steinberg H, Jarillo-Herrero P, and Gedik N 2013 *Science* **342** 453
[59] Mahmood F, Chan C K, Alpichshev Z, Gardner D, Lee Y, Lee P A, and Gedik N 2016 *Nat. Phys.* **12** 306
[60] McIver J W, Schulte B, Stein F U, Matsuyama T, Jotzu G, Meier G, and Cavalleri A 2019 *Nat. Phys.* **16** 38

[61] Zhou S H, Bao C H, Fan B S, Zhou H, Gao Q X, Zhong H Y, Lin T Y, Liu H, Yu P, Tang P Z, Meng S, Duan W H, and Zhou S Y 2023 *Nature* **614** 75

[62] He L, Addison Z, Jin J, Mele E J, Johnson S G, and Zhen B 2019 *Nat. Commun.* **10** 4194

[63] Ito S, Schüler M, Meierhofer M, Schlauderer S, Freudenstein J, Reimann J, Afanasiev D, Kokh K A, Tereshchenko O E, Güdde J, Sentef M A, Höfer U, and Huber R 2023 *Nature* **616** 696

[64] Katan Y T and Podolsky D 2013 *Phys. Rev. Lett.* **110** 016802

[65] Sun X Q, Xiao M, Bzdušek T, Zhang S C, and Fan S 2018 *Phys. Rev. Lett.* **121** 196401

[66] Lee C H, Ho W W, Yang B, Gong J, and Papić Z 2018 *Phys. Rev. Lett.* **121** 237401

[67] Chen R, Zhou B, and Xu D H 2018 *Phys. Rev. B* **97** 155152

[68] Chen R, Xu D H, and Zhou B 2018 *Phys. Rev. B* **98** 235159

[69] Nakagawa M, Slager R J, Higashikawa S, and Oka T 2020 *Phys. Rev. B* **101** 075108

[70] Zhan F Y, Ning Z, Gan L Y, Zheng B B, Fan J, and Wang R 2022 *Phys. Rev. B* **105** L081115

[71] Ning Z, Fu B, Xu D H, and Wang R 2022 *Phys. Rev. B* **105** L201114

[72] Jangjan M, Foa Torres L E F, and Hosseini M V 2022 *Phys. Rev. B* **106** 224306

[73] Qin F, Lee C H, and Chen R 2022 *Phys. Rev. B* **106** 235405

[74] Olin S and Lee W C 2023 *Phys. Rev. B* **107** 094310

[75] Wang Z M, Wang R, Sun J H, Chen T Y, and Xu D H 2023 *Phys. Rev. B* **107** L121407

[76] Qin F, Lee C H, and Chen R 2023 *Phys. Rev. B* **108** 075435

[77] Jangjan M and Hosseini M V 2020 *Sci. Rep.* **10** 14256

[78] Jangjan M and Hosseini M V 2021 *Sci. Rep.* **11** 12966

[79] Zhan F Y, Zeng J J, Chen Z, Jin X, Fan J, Chen T Y, and Wang R 2023 *Nano Lett.* **23** 2166

[80] Kolodrubetz M H, Nathan F, Gazit S, Morimoto T, and Moore J E 2018 *Phys. Rev. Lett.* **120** 150601

[81] Rudner M S, Lindner N H, Berg E, and Levin M 2013 *Phys. Rev. X* **3** 031005

[82] Kitagawa T, Oka T, Brataas A, Fu L, and Demler E 2011 *Phys. Rev. B* **84** 235108

[83] Oka T and Aoki H 2009 *Phys. Rev. B* **79** 081406

[84] Kitagawa T, Berg E, Rudner M, and Demler E 2010 *Phys. Rev. B* **82** 235114

[85] Gu Z, Fertig H A, Arovas D P, and Auerbach A 2011 *Phys. Rev. Lett.* **107** 216601

[86] Rechtsman M C, Zeuner J M, Plotnik Y, Lumer Y, Podolsky D, Dreisow F, Nolte S, Segev M, and Szameit A 2013 *Nature* **496** 196

[87] Cayssol J, Dóra B, Simon F, and Moessner R 2013 *Phys. Status Solidi RRL* **7** 101

[88] Rudner M S and Lindner N H 2020 *Nat. Rev. Phys.* **2** 229

[89] Perez-Piskunow P M, Usaj G, Balseiro C A, and Torres L E F F 2014 *Phys. Rev. B* **89** 121401

[90] Usaj G, Perez-Piskunow P M, Foa Torres L E F, and Balseiro C A 2014 *Phys. Rev. B* **90** 115423

[91] Kundu A, Fertig H A, and Seradjeh B 2014 *Phys. Rev. Lett.* **113** 236803

[92] Foa Torres L E F, Perez-Piskunow P M, Balseiro C A, and Usaj G 2014 *Phys. Rev. Lett.* **113** 266801

[93] Titum P, Lindner N H, Rechtsman M C, and Refael G 2015 *Phys. Rev. Lett.* **114** 056801

[94] Wan X L, Ning Z, Xu D H, Zheng B B, and Wang R 2023 arXiv:2307.07116v2 [cond-mat.mes-hall]

[95] Maczewsky L J, Zeuner J M, Nolte S, and Szameit A 2017 *Nat. Commun.* **8** 13756

[96] Cheng Q Q, Pan Y M, Wang H Q, Zhang C S, Yu D, Gover A, Zhang H, Li T, Zhou L, and Zhu S N 2019 *Phys. Rev. Lett.* **122** 173901

[97] Pyrialakos G G, Apostolidis A, Khajavikhan M, Kantartzis N V, and Christodoulides D N 2023 *Phys. Rev. B* **107** 174313

[98] Kitagawa T, Broome M A, Fedrizzi A, Rudner M S, Berg E, Kassal I, Aspuru-Guzik A, Demler E, and White A G 2012 *Nat. Commun.* **3** 882

[99] Mukherjee S, Spracklen A, Valiente M, Andersson E, Öhberg P, Goldman N, and Thomson R R 2017 *Nat. Commun.* **8** 13918

[100] Afzal S, Zimmerling T J, Ren Y, Perron D, and Van V 2020 *Phys. Rev. Lett.* **124** 253601

[101] Maczewsky L J, Höckendorf B, Kremer M, Biesenthal T, Heinrich M, Alvermann A, Fehske H, and Szameit A 2020 *Nat. Mater.* **19** 855

[102] Fleury R, Khanikaev A B, and Alú A 2016 *Nat. Commun.* **7** 11744

[103] Peng Y G, Qin C Z, Zhao D G, Shen Y X, Xu X Y, Bao M, Jia H, and Zhu X F 2016 *Nat. Commun.* **7** 13368

[104] Zhu W, Xue H, Gong J, Chong Y, and Zhang B 2022 *Nat. Commun.* **13** 11

[105] Cheng Z, Bomantara R W, Xue H, Zhu W, Gong J, and Zhang B 2022 *Phys. Rev. Lett.* **129** 254301

[106] Dabiri S S and Cheraghchi H 2023 *J. Appl. Phys.* **134** 084303

[107] Jotzu G, Messer M, Desbuquois R, Lebrat M, Uehlinger T, Greif D, and Esslinger T 2014 *Nature* **515** 237

[108] Asteria L, Tran D T, Ozawa T, Tarnowski M, Rem B S, Fläschner N, Sengstock K, Goldman N, and Weitenberg C 2019 *Nat. Phys.* **15** 449

[109] Wintersperger K, Braun C, Ünal F N, Eckardt A, Liberto M D, Goldman N, Bloch I, and Aidelsburger M 2020 *Nat. Phys.* **16** 1058

[110] Zhang J Y, Yi C R, Zhang L, Jiao R H, Shi K Y, Yuan H, Zhang W, Liu X J, Chen S, and Pan J W 2023 *Phys. Rev. Lett.* **130** 043201

[111] Weisbrich H, Klees R, Rastelli G, and Belzig W 2021 *PRX Quantum* **2** 010310

[112] Chen A, Guan Y, Lenggenhager P M, Maciejko J, Boettcher I, and Bzdušek T C V 2023 *Phys. Rev. B* **108** 085114

[113] Shirley J H 1965 *Phys. Rev.* **138** B979

[114] Titum P, Lindner N H, and Refael G 2017 *Phys. Rev. B* **96** 054207

[115] Liu Z R, Chen R, and Zhou B 2024 *Phys. Rev. B* **109** 125303